Journal of Fluids and Structures (2001) **15**, 207–225
doi:10.1006/jfls.2000.0335, available online at http://www.idealibrary.com on IDEAL®

UNSTEADY LIFT AND SOUND PRODUCED BY AN AIRFOIL IN A TURBULENT BOUNDARY LAYER

M. S. Howe
College of Engineering, Boston University, 110 Cummington Street, Boston, MA 02215, U.S.A.

(Received 14 December 1999, and in final form 28 September 2000)

An analysis is made of the unsteady lift exerted on a stationary rigid body immersed in an incompressible, plane-wall turbulent boundary layer. The lift is expressed as a surface integral over the body involving the *upwash* velocity induced by the "free" vorticity $\boldsymbol{\Omega}$ (found by taking explicit account of the interaction of the body with the flow and excluding the bound vorticity) and a harmonic function X_2 that depends only on the shape of the body. The upwash velocity is the free-field velocity given in terms of $\boldsymbol{\Omega}$ by the Biot–Savart formula, augmented by the velocity field of a conventional distribution of image vortices in the wall. The function X_2 can be interpreted as the velocity potential of flow past the body, produced by motion of the wall at unit speed towards the body. Detailed predictions are made of the lift on a slender airfoil placed in the outer region of the boundary-layer. When the airfoil chord is large compared to the boundary-layer thickness, vortex shedding into the wake causes the magnitude of the net upwash velocity near the trailing edge to be small. The main contributions to the surface integral are then from the nose region, where the upwash velocity may be estimated independently of the fluctuations near the trailing edge. Analytical results for a thin plate airfoil of chord $2a$ at distance h from the wall show that the lift increases as a/h increases; it is ultimately independent of a and scales with the ratio of h to the hydrodynamic wavelength. Application is made to determine the sound generated by the airfoil in a weakly compressible boundary layer flow over a finite elastic plate. © 2001 Academic Press

1. INTRODUCTION

The amplitude of the sound produced by an airfoil in a turbulent stream is proportional to unsteady lift when the Mach number is sufficiently small that the airfoil chord can be regarded as acoustically compact (Curle 1955). This important limiting case was first considered by Sears (1941), who modeled the turbulence as a "gust" in which the velocity fluctuation is a small fraction of the mean stream velocity U. Subsequent theoretical analyses have made extensive use of this approximation. The papers by Amiet & Sears (1970), Mugridge (1971), Widnall (1971), Filotas (1973), Goldstein & Atassi (1976), Howe (1976), Atassi (1984), Glegg (1989) and Marshall & Grant (1996), are typical, but represent a small fraction of the literature on this subject. The original work of Sears treated the airfoil as an isolated, two-dimensional rigid plate at zero mean angle of attack. This approximation yields predictions for the unsteady lift that are often adequate in applications, although refinements involving the modification of a turbulent eddy during convection past an airfoil of finite thickness, camber and angle of attack have also been considered [e.g. Goldstein & Atassi (1976), Atassi (1984) and Howe (1989*a*)]. These corrections are often difficult to apply in practice, however, because of gross uncertainties in the detailed properties of the impinging turbulent flow.

The principal component of the sound generated during interactions at low Mach number can be ascribed to an acoustic dipole whose strength is equal to the unsteady lift,

0889–9746/01/020207 + 19 $35.00/0 © 2001 Academic Press

and varies as Uv, where v is a characteristic turbulence velocity. The dipole axis is normal to the mean flow direction, and the amplitude of the acoustic pressure is proportional to $\rho_o vUM$, where ρ_o is the mean fluid density and $M \ll 1$ is the mean flow Mach number. The strength of the lift fluctuations and the acoustic intensity can be significantly modified (for constant turbulence inflow) when the airfoil is close to a large surface. For example, the unsteady lift is usually increased for a small airfoil deployed as a large-eddy break-up device (LEBU) in a turbulent wall boundary layer. However, if the wall is rigid the amplitude of the sound produced by the lift dipole at low Mach numbers is considerably reduced by a factor $\sim \mathcal{O}(M) \ll 1$, now varying as $\rho_o vUM^2$, because the lift dipole is cancelled by an equal and opposite image dipole in the wall. The net reduced contribution from these dipoles is comparable to the sound produced by the turbulence *quadrupole* sources in the boundary layer (Lighthill 1952). In these circumstances, Dowling (1989) has argued that the sound is dominated by the dipole radiation generated by the unsteady airfoil *drag*, whose amplitude scales as $\rho_o v^2 M$.

This conclusion, however, is strictly valid for a rigid wall. In practice, it is usually permissible to regard the wall as rigid only when the dominant scales of the motions of interest are comparable to the wall thickness, or smaller. This would be the case, for example, for the "hydrodynamic" components of the disturbance produced by a LEBU. However, the wavelength of the generated sound is typically of order $\delta/M \gg \delta$ or larger (where δ is the boundary-layer thickness), and can greatly exceed the wall thickness. Acoustic waves can then be strongly coupled to wall motions, and this can substantially *increase* the efficiency of their production by the LEBU to the extent that the amplitude of the sound becomes comparable to that of a free-field dipole ($\sim \mathcal{O}(\rho_o vUM)$) over an extensive range of frequencies (Howe 1989*b*). This is because the overall strength of the image dipole is proportional to the "reflection coefficient" of the wall, which depends on both the frequency and wavelength of the different Fourier components of the motion produced by the lift dipole; the rigid wall is a special and a typical case because the reflection coefficient is always equal to -1 irrespective of the frequency and wavelength.

In this paper, we derive a general formula for the unsteady lift experienced by a rigid airfoil placed within a wall turbulent boundary layer at very low Mach number. This formula involves the vorticity and velocity distribution in the boundary layer and wake of the airfoil and a harmonic function X_2 (solution of Laplace's equation) that depends on airfoil shape. It is shown how the lift can be expressed as a surface integral over the airfoil involving X_2 and the "upwash" velocity induced by the vorticity and its "image" distribution in the wall. The Sears formula for a two-dimensional, isolated airfoil and a two-dimensional gust can be derived as a special case. The function X_2 is just equal to the velocity potential of flow past the airfoil produced by normal motion of the wall towards the airfoil at unit speed. Particular attention is given to the case [not considered by Dowling (1989) or Howe (1989*b*)] of an airfoil whose chord is large compared to both the boundary-layer thickness and the stand-off distance from the wall. This would be relevant, for example, to problems involving the interaction of a shrouded rotor with a wall boundary layer. Gebert & Atassi (1989) have given a numerical solution of this problem for arbitrary stand-off distance and a two-dimensional gust, but their predictions at large reduced frequencies do not agree uniformly with the analytical result of this paper.

The general lift formula is discussed first for an isolated airfoil (Section 2) and then for an airfoil adjacent to a wall (Section 3). A detailed analysis is given in Section 4 for a two-dimensional, flat-plate airfoil. Application is made in Section 5 to determine the sound produced by interaction of this airfoil with boundary-layer turbulence when the boundary-layer thickness δ is small compared to the airfoil chord, and when the adjacent wall is elastic and of finite length.

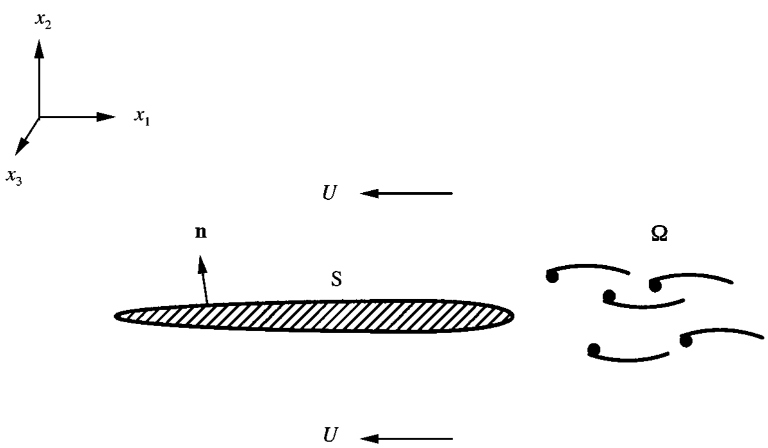

Figure 1. Isolated airfoil in a turbulent stream.

2. THE ISOLATED AIRFOIL

2.1. Gust-induced Surface Force

Consider an airfoil with surface S at rest in an incompressible turbulent stream in an unbounded fluid of uniform mean density ρ_o and shear coefficient of viscosity η (Figure 1). Let the mean flow be in the negative x_1-direction of the rectangular coordinates (x_1, x_2, x_3), with the x_2-axis vertically "upwards", in the direction of the mean lift, and x_3 in the span-wise direction. Newton's second law permits the unsteady force F_i exerted on the airfoil in the i-direction to be written,

$$F_i = -\frac{\mathrm{d}}{\mathrm{d}t}\int \rho_o v_i \,\mathrm{d}^3\mathbf{x} + \oint_\Sigma p\,\mathrm{d}S_i, \tag{2.1}$$

where $\mathbf{v}$ is the fluid velocity, p the pressure, and the volume integration is over the region of fluid V bounded internally by S and externally by a large surface Σ that may be assumed to convect with the fluid. The surface element $\mathrm{d}S_i$ on Σ is directed into V.

The size of the integration region can be significantly reduced, and the integral over Σ eliminated, by using the momentum equation,

$$\frac{\partial(\rho_o \mathbf{v})}{\partial t} + \nabla\left(p + \frac{1}{2}\rho_o v^2\right) = -\rho_o \boldsymbol{\Omega}\wedge\mathbf{v} - \eta\,\mathrm{curl}\,\boldsymbol{\Omega}, \tag{2.2}$$

where $\boldsymbol{\Omega} = \mathrm{curl}\,\mathbf{v}$ is the vorticity, to transform the right-hand side of equation (2.1) into a set of equivalent integrals confined to the turbulent region (where $\boldsymbol{\Omega} \neq \mathbf{0}$) and to the surface S. To do this, we first define the harmonic function

$$X_i = x_i - \varphi_i^*(\mathbf{x}), \tag{2.3}$$

where $\varphi_i^*(\mathbf{x})$ is the velocity potential (solution of $\nabla^2\varphi_i^* = 0$) of the ideal, incompressible flow that would be produced by rigid-body translational motion of S at unit speed in the i-direction. Then $\nabla X_i \cdot \mathbf{n} = 0$ on S, where $\mathbf{n}$ is the unit normal on S (directed into the fluid); X_i may therefore be interpreted as the velocity potential of ideal flow past the fixed airfoil in the i-direction, normalized to have unit speed at large distances from the airfoil.

Take the scalar product of ∇X_i with equation (2.2), and integrate over the fluid. The divergence theorem may now be applied [as described in detail by Howe (1989a)] to obtain an equation that expresses the right-hand side of equation (2.1) in terms of the following integrals:

$$F_i = \rho_o \int \nabla X_i \cdot \boldsymbol{\Omega} \wedge \mathbf{v} \, \mathrm{d}^3\mathbf{x} - \eta \oint_S \boldsymbol{\Omega} \wedge \nabla X_i \cdot \mathbf{n} \, \mathrm{d}S. \tag{2.4}$$

The volume integral represents the vector sum of the normal dynamic pressure force on S; the surface integral is the net effect of surface frictional forces.

2.2. Lift Represented in Terms of the Upwash Velocity

The final representation in equation (2.4) can be further reduced at very high Reynolds numbers to a single surface integral over S by introducing the "upwash" velocity induced by the vorticity $\boldsymbol{\Omega}$. If $B = p/\rho_o + \frac{1}{2}v^2$ (the total enthalpy), then the divergence of equation (2.2) supplies (for an incompressible fluid)

$$\nabla^2 B = -\operatorname{div}(\boldsymbol{\Omega} \wedge \mathbf{v}), \tag{2.5}$$

from which B can be determined when the vorticity and velocity are known. Let B_I denote the particular solution of this equation that vanishes as $|\mathbf{x}| \to \infty$ when the presence of the airfoil is ignored (although the full effect of the airfoil in determining $\boldsymbol{\Omega}$ and $\mathbf{v}$ is retained), i.e., let

$$B_I(\mathbf{x}, t) = \frac{1}{4\pi} \operatorname{div} \int \frac{(\boldsymbol{\Omega} \wedge \mathbf{v})(\mathbf{y}, t)}{|\mathbf{x} - \mathbf{y}|} \mathrm{d}^3\mathbf{y}. \tag{2.6}$$

Now, $\nabla^2 X_i = 0$ in the fluid, and it therefore follows from Green's theorem that

$$\oint_S \left(X_i \frac{\partial B_I}{\partial x_n} - B_I \frac{\partial X_i}{\partial x_n} \right) \mathrm{d}S = \int X_i \operatorname{div}(\boldsymbol{\Omega} \wedge \mathbf{v}) \, \mathrm{d}^3\mathbf{x} \equiv - \oint_S X_i (\boldsymbol{\Omega} \wedge \mathbf{v})_n \, \mathrm{d}S - \int \nabla X_i \cdot (\boldsymbol{\Omega} \wedge \mathbf{v}) \, \mathrm{d}^3\mathbf{x},$$

where the subscript n for a vector quantity evaluated on S denotes the normal component directed *into* the fluid. Because $\partial X_i / \partial x_n \equiv 0$, this result may be rearranged into the form

$$\int \nabla X_i \cdot (\boldsymbol{\Omega} \wedge \mathbf{v}) \, \mathrm{d}^3\mathbf{x} = - \oint_S X_i \left(\frac{\partial B_I}{\partial x_n} + (\boldsymbol{\Omega} \wedge \mathbf{v})_n \right) \mathrm{d}S. \tag{2.7}$$

The integrand on the right is transformed further by taking the gradient of equation (2.6) and using the identities $\nabla \operatorname{div} = \operatorname{curl} \operatorname{curl} + \nabla^2$ and $\nabla^2 (1/|\mathbf{x} - \mathbf{y}|) = -4\pi \, \delta(\mathbf{x} - \mathbf{y})$, to show that

$$\nabla B_I + \boldsymbol{\Omega} \wedge \mathbf{v} = \operatorname{curl} \int \frac{\operatorname{curl}(\boldsymbol{\Omega} \wedge \mathbf{v})(\mathbf{y}, t)}{4\pi |\mathbf{x} - \mathbf{y}|} \mathrm{d}^3\mathbf{y}. \tag{2.8}$$

This result is used to define the *upwash* velocity $\mathbf{v}_I$ by

$$\frac{\partial \mathbf{v}_I}{\partial t} = - \operatorname{curl} \int \frac{\operatorname{curl}(\boldsymbol{\Omega} \wedge \mathbf{v})(\mathbf{y}, t)}{4\pi |\mathbf{x} - \mathbf{y}|} \mathrm{d}^3\mathbf{y}. \tag{2.9}$$

The limiting value of $\mathbf{v}_I$ as the Reynolds number tends to infinity corresponds to the induced velocity of the "free" vorticity, i.e., the total vorticity excluding *bound vorticity* on the airfoil. Indeed, by integration of the vorticity equation [the curl of equation (2.2)] we find

$$\int \frac{\operatorname{curl}(\boldsymbol{\Omega} \wedge \mathbf{v})}{4\pi |\mathbf{x} - \mathbf{y}|} \mathrm{d}^3\mathbf{y} = - \int \left(\frac{\partial \boldsymbol{\Omega}}{\partial t} - \nu \nabla^2 \boldsymbol{\Omega} \right) \frac{\mathrm{d}^3\mathbf{y}}{4\pi |\mathbf{x} - \mathbf{y}|},$$

where $v = \eta/\rho_o$ is the kinematic viscosity. At high Reynolds numbers the vorticity diffusion term $v\nabla^2\mathbf{\Omega}$ is negligible except within the viscous sublayer on the airfoil where, however, the motion becomes linear and $\partial\mathbf{\Omega}/\partial t - v\nabla^2\mathbf{\Omega} \to 0$. Equation (2.9) is then equivalent to the *Biot–Savart* induction formula (Batchelor 1967)

$$\mathbf{v}_I(\mathbf{x}, t) = \operatorname{curl} \int_{V_\delta} \frac{\mathbf{\Omega}(\mathbf{y}, t)\,\mathrm{d}^3\mathbf{y}}{4\pi|\mathbf{x} - \mathbf{y}|}, \tag{2.10}$$

where the integration is confined to the region V_δ occupied by the free vorticity *outside* the viscous sublayer on the airfoil. The latter restriction confirms that when the Reynolds number is large enough that the motion is effectively inviscid except within an infinitesimal distance from the surface of airfoil, contributions to integral (2.10) from *bound* vorticity on S must be ignored.

Equations (2.4) and (2.7) therefore permit the surface force to be expressed in the form

$$F_i = \rho_o \oint_S X_i \frac{\partial v_{In}}{\partial t}\,\mathrm{d}S - \eta \oint_S \mathbf{\Omega} \wedge \nabla X_i \cdot \mathbf{n}\,\mathrm{d}S. \tag{2.11}$$

In particular, when the Reynolds number is sufficiently large that frictional surface stresses may be ignored, the unsteady lift force F_2 becomes

$$F_2 = \rho_o \oint_S X_2 \frac{\partial v_{In}}{\partial t}\,\mathrm{d}S. \tag{2.12}$$

2.3. Gust-induced Lift for a Thin Plate Airfoil

Consider the special case illustrated in Figure 2 of a two-dimensional airfoil consisting of a rigid strip of chord $2a$ set at zero angle of attack to the mean flow. Let the airfoil occupy $-a < x_1 < a$, $x_2 = 0$, $-\infty < x_3 < \infty$, and suppose a small amplitude, two-dimensional time harmonic gust of frequency ω (proportional to $\mathrm{e}^{-i\omega t}$) is incident from upstream ($x_1 = +\infty$). In the *absence* of the airfoil, and assuming that the gust is passively convected along by the mean flow, this would generate an upwash velocity in the plane $x_2 = 0$ whose "vertical" component is, say,

$$v_2 = v(\omega)\mathrm{e}^{-i\omega(t + x_1/U)}, \tag{2.13}$$

where $v(\omega)$ may be regarded as known.

According to Sears (1941), the unsteady, high Reynolds number lift *per unit span* $F_2(\omega)\mathrm{e}^{-i\omega t}$ produced by the gust is given by

$$F_2(\omega) = 2\pi a \rho_o v(\omega) U \mathscr{S}\left(\frac{\omega a}{U}\right), \qquad \mathscr{S}(x) = \frac{2}{\pi x(\mathrm{H}_0^{(1)}(x) + i\mathrm{H}_1^{(1)}(x))}, \tag{2.14}$$

where $\mathscr{S}$ is the *Sears function*, and $\mathrm{H}_0^{(1)}$, $\mathrm{H}_1^{(1)}$ are Hankel functions (Abramowitz & Stegun 1970). The real and imaginary parts of $\mathscr{S}$ are plotted as the solid curves in Figure 2 as functions of the reduced frequency $\omega a/U$.

In order to derive the Sears result (2.14) from the general formula (2.12) it is not sufficient to take v_{In} to be defined by the upwash velocity (2.13) induced by the gust, because the interaction of the airfoil with the gust produces new vorticity shed into the wake. This vorticity is necessary to ensure that the flow leaves the trailing edge smoothly, in accordance with the Kutta condition (Crighton 1985). But this also means that the overall importance of the trailing edge region as a source of unsteady lift is significantly diminished. Indeed, when the reduced frequency $\omega a/U > 1$, it is a very good approximation to assume that the

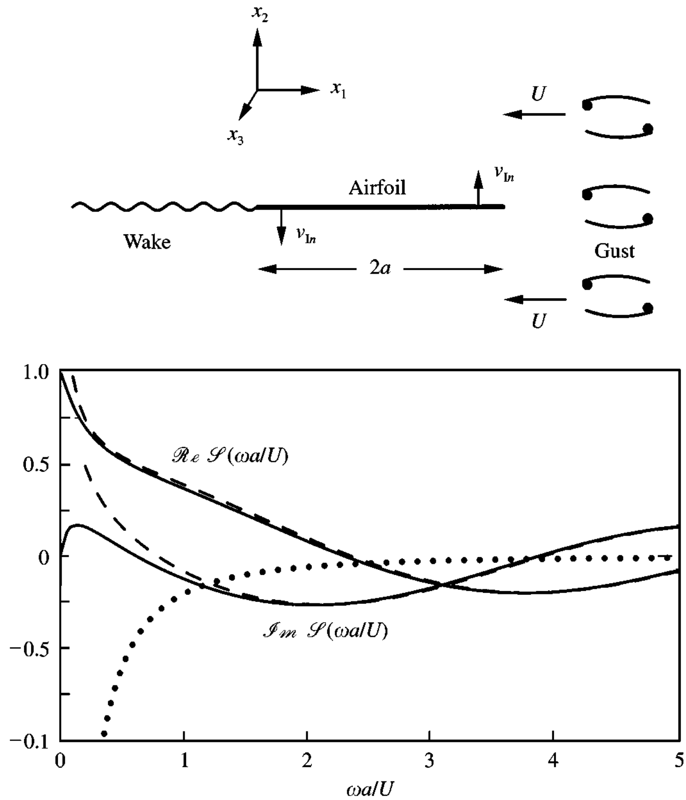

Figure 2. Comparison of the exact formula (2·14) (——) and the asymptotic formula (2·16) (— — —) for the lift on a two-dimensional airfoil; • • •, ratio (in dB) of the corresponding mean square lift forces.

net value of the *total* upwash velocity v_{In} becomes negligible near the trailing edge, where the component produced by the wake vorticity is effectively equal and opposite to component (2.13) produced by the gust alone. Near the leading edge, however, the influence of the wake is negligible, and v_{In} can be approximated by equation (2.13).

Thus, for $\omega a/U > 1$ the lift can be evaluated from equation (2.12) by taking v_{In} to be given by equation (2.13) and confining the integration to the region close to the leading edge. To do this note first that (Batchelor 1967)

$$\begin{aligned} X_2 &= \mathscr{R}e(-\mathrm{i}\sqrt{z^2 - a^2}), \quad \text{where } z = x_1 + \mathrm{i}x_2, \\ &\approx \mathscr{R}e(-\mathrm{i}\sqrt{2a}\sqrt{z-a}) \quad \text{near the leading edge.} \end{aligned} \tag{2.15}$$

Then equation (2.12) is approximated as follows, by expanding the integrand about the leading edge of the airfoil:

$$\begin{aligned} F_2(\omega) = -\mathrm{i}\omega\rho_o \oint_S X_2 v_{In}(\omega)\,\mathrm{d}S &\approx -2\mathrm{i}\omega\rho_o \int_{-\infty}^{a} v(\omega)\mathrm{e}^{-\mathrm{i}\omega x_1/U}\sqrt{2a(a-x_1)}\,\mathrm{d}x_1 \\ &= 2\pi a\rho_o v(\omega)U\left[\frac{\mathrm{e}^{\mathrm{i}(\pi/4)-(\omega a/U)}}{\sqrt{2\pi(\omega a/U)}}\right]. \end{aligned} \tag{2.16}$$

This should be compared with the exact formula (2.14). The quantity in the square brackets in the last line of equation (2.16) replaces the Sears function of equation (2.14); it is readily confirmed to be identical to the limiting value of $\mathscr{S}(\omega a/U)$ as $\omega a/U \to \infty$. Its real and imaginary parts are plotted as the broken line curves in Figure 2. Significant differences between the exact and approximate values are evident only for $\omega a/U < 1$, and this confirms the hypothesis used in deriving equation (2.16) that, when $\omega a/U > 1$, the role of vortex shedding (i.e., of the *Kutta condition*) is to effectively reduce to zero the magnitude of the upwash velocity near the trailing edge.

The dotted curve in the figure represents the variation of

$$10 \times \log_{10}\left| 2\pi \frac{\omega a}{U} \mathscr{S}^2\left(\frac{\omega a}{U}\right)\right|.$$

This represents on a dB-scale the difference between the exact and approximate values of $|F_2(\omega)|^2$. The fact that the exact and approximate values of $|F_2(\omega)|^2$ differ by less than $\frac{1}{2}$ dB when $\omega a/U > \frac{1}{2}$ implies that an error of the same magnitude will be incurred when the approximate lift formula is used to estimate gust-generated aerodynamic sound at very low Mach number for these reduced frequencies.

3. AIRFOIL IN A TURBULENT BOUNDARY LAYER

Consider next the case of an airfoil fixed within a wall boundary layer. Assume the airfoil, the mean flow, and the coordinate system to be orientated as in Section 2, with the addition of a plane rigid wall, which is taken to coincide with the plane $x_2 = 0$ (Figure 3).

The lift F_2 on the airfoil is given by

$$F_2 = -\frac{\mathrm{d}}{\mathrm{d}t}\int \rho_o v_2 \,\mathrm{d}^3\mathbf{x} + \oint_\Sigma p \,\mathrm{d}S_2, \tag{3.1}$$

where the volume integral is over the fluid region $x_2 > 0$, and the surface integral now includes a contribution from the wall $x_2 = 0$ which gives the net normal force exerted on the fluid by the wall.

The integrals in equation (3.1) can be transformed by the method of Section 2 to give

$$F_2 = \rho_o \int \nabla X_2 \cdot \mathbf{\Omega} \wedge \mathbf{v} \,\mathrm{d}^3\mathbf{x} - \eta \oint_S \mathbf{\Omega} \wedge \nabla X_2 \cdot \mathbf{n} \,\mathrm{d}S, \tag{3.2}$$

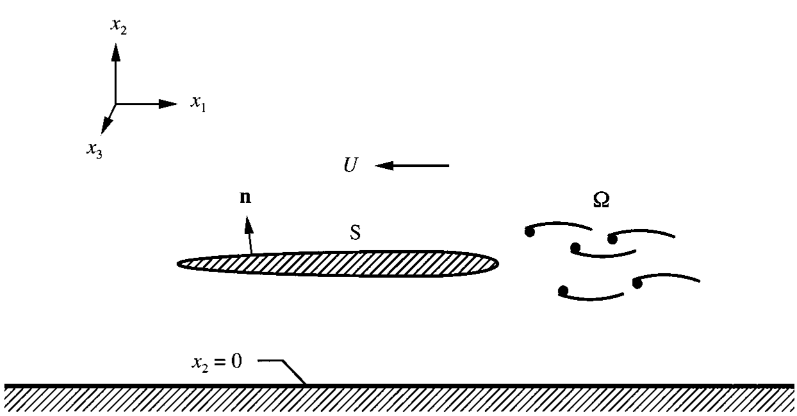

Figure 3. Airfoil in a plane-wall turbulent boundary layer.

provided the harmonic function $X_2 = x_2 - \varphi_2^*(\mathbf{x})$ is modified to satisfy

$$\begin{aligned} \partial X_2/\partial x_n &= 0, \quad \text{on the airfoil S}, \\ \partial X_2/\partial x_2 &= 1, \quad \text{on the wall } x_2 = 0. \end{aligned} \tag{3.3}$$

X_2 is now equivalent to the velocity potential of the flow past the fixed airfoil that would be produced by motion of the wall at unit speed in the x_2-direction. Equation (3.2) is formally identical to the $i = 2$ component of equation (2.4). A similar formula can be obtained for the directions $i = 1, 3$ parallel to the wall, with X_i defined as in Section 2, but in these cases F_i would represent the force on the airfoil *plus* the skin friction on the wall (the surface integral would then be taken over the airfoil *and* the wall).

Further reduction of equation (3.2) to the form (2.11) (with $i = 2$) or equation (2.12) involving the upwash velocity $\mathbf{v}_\mathrm{I}$ is achieved by introducing the following modification to definition (2.6) of B_I:

$$B_\mathrm{I}(\mathbf{x}, t) = \frac{1}{4\pi} \operatorname{div} \int_{y_2 > 0} \frac{(\boldsymbol{\Omega} \wedge \mathbf{v})(\mathbf{y}, t)}{|\mathbf{x} - \mathbf{y}|} \mathrm{d}^3\mathbf{y} - \Phi'(\mathbf{x}, t), \tag{3.4}$$

where Φ' satisfies $\nabla^2 \Phi' = 0$, $\Phi' \to 0$ as $|\mathbf{x}| \to \infty$ in $x_2 > 0$, and is chosen to make $\partial B_\mathrm{I}/\partial x_2 = 0$ on the wall $x_2 = 0$. The function Φ' therefore corresponds to the potential flow produced by a system of image vortices in the wall. The high Reynolds number formula for the lift force then becomes

$$F_2 = \rho_o \oint_S X_2 \frac{\partial v_{\mathrm{I}n}}{\partial t} \mathrm{d}S, \tag{3.5}$$

where

$$\mathbf{v}_\mathrm{I}(\mathbf{x}, t) = \operatorname{curl} \int_{\mathrm{V}_\delta} \frac{\boldsymbol{\Omega}(\mathbf{y}, t)\, \mathrm{d}^3\mathbf{y}}{4\pi|\mathbf{x} - \mathbf{y}|} + \boldsymbol{\nabla}\Phi(\mathbf{x}, t), \quad \Phi(\mathbf{x}, t) = \int_{-\infty}^{t} \Phi'(\mathbf{x}, \tau)\, \mathrm{d}\tau.$$

The upwash velocity therefore consists of the velocity induced (according to the Biot–Savart law) by the free vorticity, together with a correction that corresponds to the potential flow velocity generated by the image of the turbulent stream in the wall. In other words, the upwash velocity in the fully turbulent region of the boundary layer is precisely the velocity that would be measured in the absence of the airfoil (but when its contributions to vorticity production and convection are retained).

4. THE THIN PLATE AIRFOIL

Specific analytical results will next be derived for a thin plate airfoil of chord $2a$ adjacent to a rigid wall. A case of practical importance arises when the airfoil is located in the outer region of a boundary layer, at a stand-off distance from the wall $h \approx \delta$ = boundary-layer thickness. The numerical results of Section 2.3 indicate that the lift fluctuations at reduced frequencies $\omega a/U > 1$ can be determined to an excellent approximation by taking the upwash velocity to coincide with the velocity field of the boundary layer in the absence of the airfoil, and by limiting the integration in the surface integral (3.5) to the leading edge region (contributions from the trailing edge being suppressed by the Kutta condition). If the airfoil is taken to occupy $-a < x_1 < a$, $x_2 = h$, $-\infty < x_3 < \infty$, the potential function $X_2(\mathbf{x})$ must therefore be expanded about the leading edge $x_1 = a$, $x_2 = h$, where it will exhibit a square root singularity of the same type as in equation (2.15).

4.1. Evaluation of $X_2(\mathbf{x})$

An analytical approximation for X_2 was derived by Howe (1989*a*) for the case where a/h is small. The calculation was based on the method described by Milne-Thomson (1968) for determining the potential flow generated by a moving sphere near a rigid wall. Let $w(z)$ be the complex potential of the motion produced when the wall advances towards the stationary airfoil at unit speed, where $z = x_1 + \mathrm{i}x_2$. Then $X_2 = \mathrm{Re}\, w(z)$, and in the first Milne-Thomson approximation

$$w \approx -\mathrm{i}z + \alpha\{-\mathrm{i}\sqrt{(z-\mathrm{i}h)^2 - a^2} + \mathrm{i}\sqrt{(z+\mathrm{i}h)^2 - a^2}\}, \qquad a \ll h, \tag{4.1}$$

where α is a real coefficient to be determined. The terms in the brace brackets, respectively, correspond to the velocity potentials of flow in the x_2-direction past the airfoil when the presence of the wall is ignored, and flow *in the opposite direction* past the image of the airfoil in the wall. This formula satisfies $-\mathrm{Im}\, \mathrm{d}w/\mathrm{d}z \equiv \partial X_2/\partial x_2 = 1$ on the wall $x_2 = 0$, but $\partial X_2/\partial x_n \neq 0$ on S. In a first approximation, for $a \ll h$, the coefficient α can be chosen to make $\partial X_2/\partial x_n = \pm\, \partial X_2/\partial x_2 = 0$ along the axis of symmetry $z = \mathrm{i}\,(h \pm 0)$ of the airfoil, when it is found that

$$\alpha = f_1\left(\frac{a}{h}\right) \equiv \sqrt{1 + \frac{a^2}{4h^2}}, \qquad \frac{a}{h} \ll 1. \tag{4.2}$$

Alternatively, α can be estimated by requiring that the *average* value

$$\frac{1}{2a}\int_{-a}^{a} \frac{\partial X_2}{\partial x_2}\, \mathrm{d}x_1 = 0 \quad \text{on S}.$$

This yields

$$\alpha = f_2\left(\frac{a}{h}\right) \equiv \frac{1}{\sqrt{2}}\left(1 + \sqrt{1 + \frac{a^2}{h^2}}\right)^{1/2}, \quad \frac{a}{h} \ll 1. \tag{4.3}$$

In either case, the behavior of X_2 near the leading edge ($z = a + \mathrm{i}h$) is found to be given by

$$X_2 \approx f\left(\frac{a}{h}\right)\mathscr{Re}\{-\mathrm{i}\sqrt{2a}\sqrt{z - (a + \mathrm{i}h)}\}, \tag{4.4}$$

where $f \approx f_1, f_2$ when a/h is small. The functions f_1, f_2 are shown plotted against a/h in Figure 4 (the broken-line curves).

A more precise evaluation of X_2 and $f(a/h)$ is necessary when the airfoil chord is much larger than the stand-off distance h. This can be accomplished by means of the conformal transformation illustrated in Figure 5, where [Figure 5(a)] it is required to determine the velocity potential $X_2 \equiv X_2(z)$ ($z = x_1 + \mathrm{i}x_2$) when the wall advances towards the airfoil at unit speed. The fluid motion is evidently symmetric with respect to the x_2-axis, and the problem of calculating the ideal flow in the first quadrant of the z-plane ($x_1 > 0$) is equivalent to that depicted in Figure 5(b), where the imaginary axis is replaced by a rigid barrier and a line source of unit strength per unit length is distributed along the positive real axis ($0 < x_1 < \infty$) between O and C_∞. The lower and upper surfaces of the "positive" half of the airfoil are denoted, respectively, by BA and DA.

The complex potential $w(z)$ of the flow produced by the line source is found by mapping the first quadrant of the z-plane, cut along the segment between $z = \mathrm{i}h$ and $z = a + \mathrm{i}h$ occupied by the positive half of the airfoil, onto the *second quadrant* of the ζ-plane by means

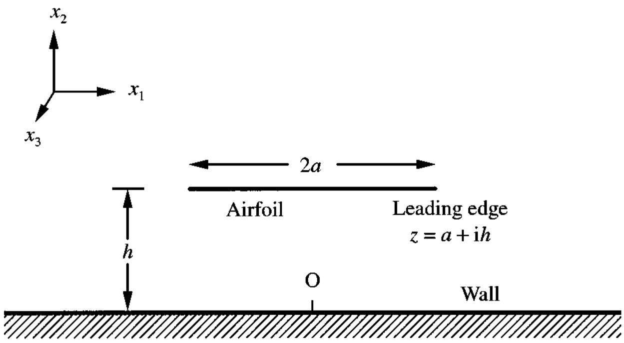

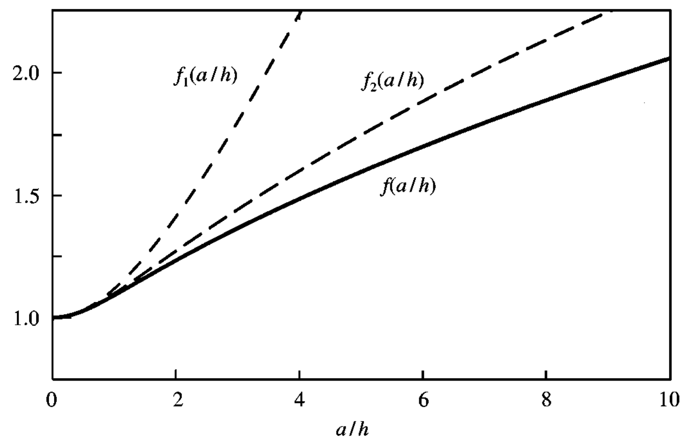

Figure 4. Plots of $f(a/h)$ and the small argument approximations f_1, f_2.

of the Schwarz–Christoffel transformation (Lamb 1932; Milne-Thomson 1968; Ivanov & Trubetskov 1995)

$$\frac{z}{h} = \frac{-\,\mathrm{i}\{\mathscr{E}(\zeta,\wp) - \chi\mathscr{F}(\zeta,\wp)\}}{E(\wp) - \chi K(\wp)}, \tag{4.5}$$

where

$$\chi = 1 - \frac{E(\wp')}{K(\wp')}, \quad \wp' = 1 - \wp, \quad 0 \le \wp < 1.$$

$\mathscr{F}(\zeta,\wp)$, $\mathscr{E}(\zeta,\wp)$ are elliptic integrals of the first and second kind, respectively (Abramowitz & Stegun 1970):

$$\mathscr{F}(\zeta,\wp) = \int_0^\zeta \frac{\mathrm{d}t}{\sqrt{1-t^2}\sqrt{1-\wp t^2}}, \quad \mathscr{E}(\zeta,\wp) = \int_0^\zeta \frac{\sqrt{1-\wp t^2}\,\mathrm{d}t}{\sqrt{1-t^2}}, \quad \mathscr{I}m\,\zeta \ge 0 \tag{4.6}$$

and $K(\wp) = \mathscr{F}(1,\wp)$, $E(\wp) = \mathscr{E}(1,\wp)$ are the corresponding complete elliptic integrals.

The images in the ζ-plane of the points labeled in Figure 5(b) are shown in Figure 5(c) and listed in Table 1.

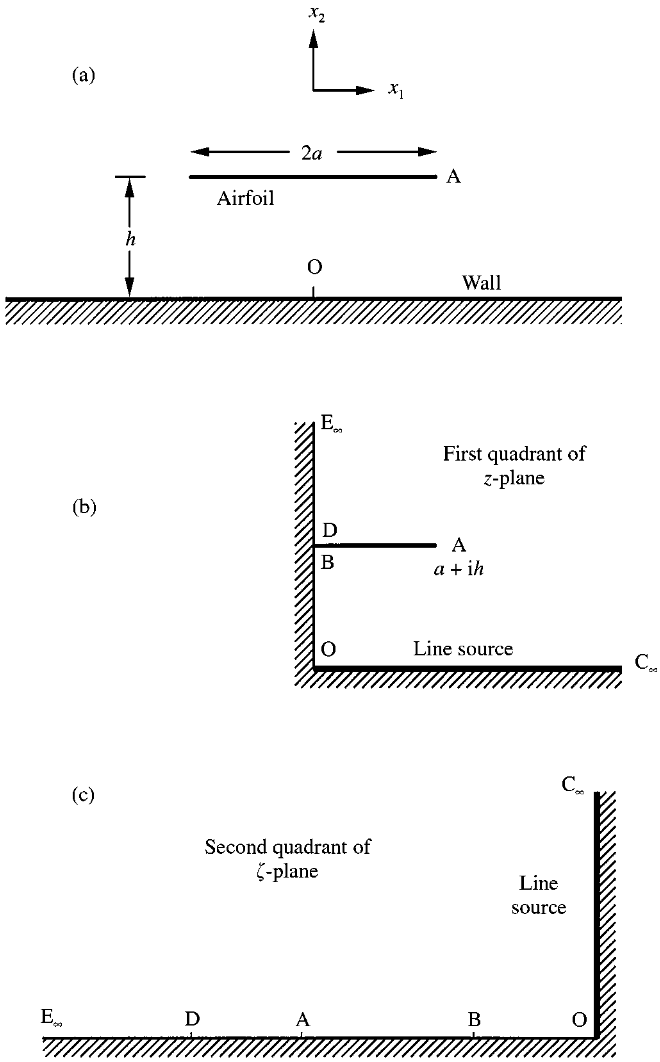

Figure 5. (a) Calculation of X_2 for arbitrary values of a/h; (b) unit strength line source and rigid barrier used to determine X_2 in the first quadrant; (c) images in the ζ-plane.

TABLE 1

Point	Image in ζ-plane
C_∞	$+\mathrm{i}\,\infty$ on the imaginary axis
B	-1
A	$-\zeta_A$, where $\zeta_A = \sqrt{E(\wp')/\wp K(\wp')}$
D	$-1/\sqrt{\wp}$
E_∞	$-\infty$ on the real axis

The condition that $\zeta = -\zeta_A$ should be the image of the airfoil leading edge $z = a + ih$ yields the relation

$$\frac{a}{h} = \frac{1}{[E(\wp) - \chi K(\wp)]}\int_1^{\zeta_A} \frac{(1 - \wp t^2 - \chi)\,dt}{\sqrt{(t^2 - 1)(1 - \wp t^2)}}, \tag{4.7}$$

which determines the value of the parameter $\wp$ in terms of a/h.

The uniform source density of unit strength along the positive real axis in the z-plane maps into a source distribution of density

$$\frac{h}{E(\wp) - \chi K(\wp)}\left(\sqrt{\frac{1 + \wp\lambda^2}{1 + \lambda^2}} - \frac{\chi}{\sqrt{(1 + \lambda^2)(1 + \wp\lambda^2)}}\right)$$

on the positive imaginary axis $\mathscr{I}m\,\zeta = \lambda$. The velocity potential in $\mathrm{Re}\,\zeta < 0$, $\mathscr{I}m\,\zeta > 0$ is therefore given by

$$w = \frac{h}{\pi[E(\wp) - \chi K(\wp)]}\int_0^{\infty} \frac{(1 + \wp\lambda^2 - \chi)\ln(\zeta^2 + \lambda^2)\,d\lambda}{\sqrt{(1 + \lambda^2)(1 + \wp\lambda^2)}}. \tag{4.8}$$

This integral is formally divergent because it includes an "infinite constant", but its derivative $dw/d\zeta$ converges and correctly determines ∇X_2 in the region $x_1, x_2 > 0$.

It follows by expanding about $\zeta = -\zeta_A$, that the behavior of $X_2 = \mathrm{Re}\,w(z)$ near the leading edge A is given by the general formula (4.4), where

$$f\left(\frac{a}{h}\right) = \frac{1}{\pi}\sqrt{\frac{h}{a}}\left[\frac{2\chi^{1/2}\zeta_A\sqrt{\zeta_A^2 - 1}}{\wp[E(\wp) - \chi K(\wp)]}\right]^{1/2}\int_0^{\infty}\frac{(1 + \wp\lambda^2 - \chi)}{\sqrt{(1 + \lambda^2)(1 + \wp\lambda^2)}}\frac{d\lambda}{(\zeta_A^2 + \lambda^2)}. \tag{4.9}$$

The right-hand side of this formula is a function of a/h alone, because $\wp$ is given in terms of a/h by equation (4.7), and $\zeta_A = \sqrt{E(\wp')/\wp K(\wp')}$. However, the integrals in equations (4.7) and (4.9) must be evaluated numerically, and it is therefore convenient first to calculate the respective parametric dependencies of $f(a/h)$ and a/h on $\wp$. The solid curve in Figure 4 is the plot of $f(a/h)$ against a/h obtained in this way.

Large values of a/h correspond to $\wp \to 0$; equations (4.7) and (4.9) can then be used to show that

$$f\left(\frac{a}{h}\right) \sim \sqrt{\frac{a}{\pi h}} \quad \text{as} \quad \frac{a}{h} \to \infty. \tag{4.10}$$

However, this asymptotic dependence is approached only when a/h is much larger than the maximum value occurring in Figure 4. For practical purposes the following modification of the small a/h formula (4.3) provides an excellent representation of $f(a/h)$ for $a/h \le 10$:

$$f\left(\frac{a}{h}\right) \approx \frac{1}{\sqrt{2}}\left[1 + \left(1 + \frac{(a/h)^2}{1 + 0{\cdot}13(a/h) - 0{\cdot}0045(a/h)^2}\right)^{1/2}\right]^{1/2}, \qquad 0 \le \frac{a}{h} \le 10. \tag{4.11}$$

4.2. The Unsteady Lift

When the characteristic scale of the upwash velocity is small compared to the airfoil chord, the main contribution to the lift force integral of equation (3.5) is from the neighborhood of the leading edge of the airfoil, where X_2 is given by equation (4.4). The leading edge singularity is the same as in equation (2.15) for the isolated airfoil (the leading edge being at

$z = a$ in Section 2). Thus, the factor $f(a/h)$ is equal to the ratio of the boundary-layer-induced lift force to the lift produced by the same impinging upwash velocity in the absence of the wall.

For the particular case of the two-dimensional, time-harmonic upwash velocity (2.13), where $\omega a/U > 1$, the lift is calculated as in equation (2.16) of Section 2.3, leading to

$$F_2(\omega) = -\mathrm{i}\omega\rho_o \oint_S X_2 v_{\mathrm{I}n}(\omega)\,\mathrm{d}S \approx 2\pi a\rho_o v(\omega)Uf\left(\frac{a}{h}\right)\left[\frac{\mathrm{e}^{\mathrm{i}(\pi/4-\omega a/U)}}{\sqrt{2\pi(\omega a/U)}}\right]. \tag{4.12}$$

When a/h is small, $f \sim 1$, and this is identical with the result (2.16) for an isolated airfoil, for which $|F_2/2a\rho_o vU|^2 \sim 1/\kappa a$, $(\kappa = \omega/U)$. Figure 4 shows how the magnitude of the lift increases (for fixed $v(\omega)$ and κa) as a/h increases. When a/h is very large $f \sim \sqrt{a/\pi h}$ and $|F_2/2a\rho_o vU|^2 \sim 1/\kappa h$, i.e., the relevant length scale determining the decrease in the lift force with increasing gust wavenumber κ is ultimately equal to the stand-off distance h rather than the airfoil chord. This conclusion is at variance with that of Gebert & Atassi [1989, equation (28)]. They find the lift to be independent of h and equal to that for an isolated airfoil for all values of a/h when $\kappa a \gg 1$, apparently because it was assumed that large values of κa also implies that $\kappa h \gg 1$. But this is only true provided that h/a is *not* small. Thus, the amplitude of our high-frequency prediction exceeds that of Gebert & Atassi (1989) by the factor $f(a/h)$ plotted in Figure 4.

5. Sound Generated by Lift Fluctuations

In flow at very low Mach number the sound attributable to an airfoil in a turbulent boundary layer is governed by the following compressible version of equation (2.5) (Howe 1998):

$$\left(\frac{1}{c_o^2}\frac{\partial^2}{\partial t^2} - \nabla^2\right)B = \mathrm{div}\,(\mathbf{\Omega} \wedge \mathbf{v}), \tag{5.1}$$

where c_o denotes the speed of sound. At large distances from the airfoil, in the acoustic far field, the acoustic pressure $p \approx \rho_o B$, where B is the perturbation value of the total enthalpy determined by equation (5.1). The turbulence source on the right of equation (5.1) produces an unsteady lift on the airfoil that is equivalent to an acoustic dipole. If the airfoil is adjacent to a large *rigid* wall, an equal and opposite image dipole is also created in the wall, and the overall radiation is equivalent to that produced by a much weaker quadrupole (see Section 1). However, a real *elastic* wall can be highly compliant at the large length scales associated with acoustic waves (especially in water), even though its behavior is effectively rigid on a scale of the hydrodynamic components of the motion. In other words, the hydrodynamic motion produced by the airfoil is typically identical to that for a rigid wall, while the wall is compliant over longer distances comparable to the acoustic wavelength. This suggests that to calculate the radiation, the force exerted on the wall should first be determined as if the motion were incompressible and the wall rigid; the acoustic field produced by this force is then found by including the influence of wall-compliance. However, to avoid any possible misunderstanding, we shall adopt the alternative procedure of first calculating the Green's function describing the radiation from sources in the neighborhood of the airfoil. A problem of this type is discussed by Howe (1989*b*) when the wall consists of an infinite elastic plate. Here we shall consider the situation illustrated in Figure 6(a), in which a two-dimensional airfoil is fixed in a boundary layer flow over a two-dimensional elastic plate of width $2\ell \gg 2a$, and where the Mach number $M = U/c_o$ is sufficiently small that the dominant acoustic wavelengths are large compared to ℓ.

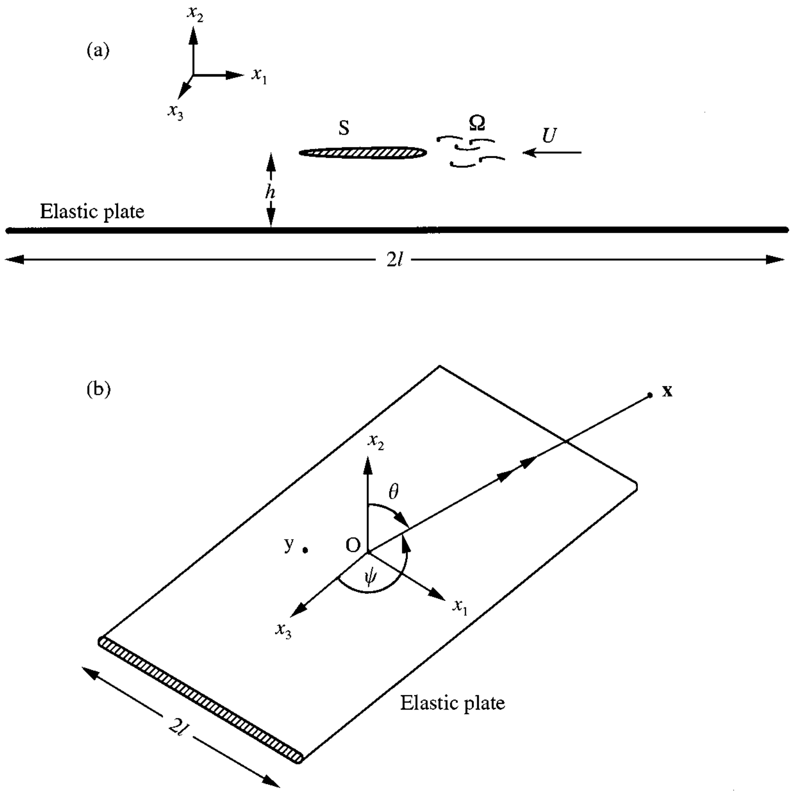

Figure 6. (a) Airfoil adjacent to a large, two-dimensional elastic plate of width 2ℓ in the presence of a turbulent boundary layer flow; (b) coordinate system used to specify the position **x** of an observer in the acoustic far field.

5.1. The Acoustic Green's Function

In these circumstances Green's function G for the acoustic problem can readily be derived for each frequency component (proportional to $\mathrm{e}^{-\mathrm{i}\omega t}$) of the radiation. If $\nabla_{\mathbf{y}}^2$ is the Laplacian with respect to **y**, and the observer is at **x** in the acoustic far field [see Figure 6(b)], $G = G(\mathbf{x}, \mathbf{y}, \omega)$ may be regarded as the velocity potential determined as a function of **y** by the reciprocal problem

$$(\nabla_y^2 + k_o^2)G = \delta(\mathbf{y} - \mathbf{x}), \tag{5.2}$$

in which the spherical wave

$$G_o = \frac{-\,\mathrm{e}^{\mathrm{i}k_o|\mathbf{y}-\mathbf{x}|}}{4\pi|\mathbf{y} - \mathbf{x}|} \tag{5.3}$$

generated by the point source at **x** [on the right of equation (5.2)] is diffracted by the elastic plate and by the airfoil.

To calculate G near the plate it is necessary to determine the motion of the plate produced by this spherical wave. In a first approximation (for $a \ll \ell$), we can neglect the influence of the airfoil in calculating the plate motion. Thus, ignoring for the moment the presence of the airfoil, we write

$$G = G_o + G_s, \tag{5.4}$$

where G_s denotes the field diffracted by the plate. Near the plate

$$G_o \approx \mathscr{A}(1 - \mathrm{i}k_o y_2 \cos\Theta), \qquad \mathscr{A} = \frac{-\,\mathrm{e}^{\mathrm{i}k_o|\mathbf{x}| - \mathrm{i}k_3 y_3}}{4\pi|\mathbf{x}|}, \quad |\mathbf{x}| \to \infty, \qquad k_o y_2 \ll 1, \tag{5.5}$$

where $k_3 = k_o \cos\psi$; the angles ψ, Θ define the orientation of the observer direction $\mathbf{x}$, and coordinate axes are taken as in Figure 6(b), with the origin O on the centerline of the plate.

To determine the corresponding approximation for G_s near the plate, note that the motion of the plate produced by the incident wave G_o must be independent of y_1 when $k_o\ell$ is small, i.e., its normal velocity $\mathscr{V} = \mathscr{V}(y_3)$ is a function only of the span-wise coordinate y_3. At large distances from the plate G_s must therefore represent the field of an outgoing *line dipole*, proportional to

$$\mathrm{H}_1^{(1)}(\bar{k}_o r)\sin\theta\,\mathrm{e}^{-\mathrm{i}k_3 y_3}, \qquad \bar{k}_o = \sqrt{k_o^2 - k_3^2} = k_o \sin\psi,$$

where (r, θ) are polar coordinates, defined such that $(y_1, y_2) = r(\cos\theta, \sin\theta)$. The lowest-order terms in the small argument expansion of the Hankel function are local solutions of Laplace's equation, and we can accordingly write, in the immediate vicinity of the plate,

$$\begin{aligned} G_s \approx\; & -\mathrm{i}Ak_o\cos\Theta\,\mathrm{Re}(-\mathrm{i}\sqrt{z^2-\ell^2} + \mathrm{i}z) \\ & + \mathscr{V}\mathrm{Re}(\mathrm{i}\sqrt{z^2-\ell^2} - \mathrm{i}z) + \frac{\mathrm{i}\pi(\bar{k}_o\ell)^2}{8}\mathscr{V}\mathrm{Re}(\mathrm{i}\sqrt{z^2-\ell^2}), \quad z = y_1 + \mathrm{i}y_2. \end{aligned} \tag{5.6}$$

The combination of the first term on the right of equation (5.6) with the incident wave represents a disturbance whose normal velocity vanishes on the plate. The second term represents the local incompressible motion produced by the oscillatory motion of the plate at normal velocity $\mathscr{V}$, and the final term (which differs in phase by 90°) represents the leading order near-field term involving fluid compressibility. The latter governs the influence of radiation damping on the motion of the plate, and is required to ensure that $\mathscr{V}$ remains finite when the plate is excited at the *coincidence frequency* (Junger & Feit 1993).

If D and m, respectively, denote the bending stiffness and mass per unit area of the plate, $\mathscr{V}$ satisfies the bending wave equation

$$\left(D\frac{\mathrm{d}^4}{\mathrm{d}y_3^4} - m\omega^2\right)\mathscr{V} = -\mathrm{i}\omega\int_{-\ell}^{\ell}[p(y_1, -0, y_3) - p(y_1, +0, y_3)]\,\mathrm{d}y_1, \tag{5.7}$$

where the pressure is given by the linearized relation $p = \mathrm{i}\omega\rho_o(G_o + G_s)$, and the pressure loading is therefore calculated from equation (5.6) to be

$$p(y_1, -0, y_3) - p(y_1, +0, y_3) = -2\rho_o\omega\left\{\mathscr{A}k_o\cos\Theta - \mathrm{i}\mathscr{V}\left(1 + \frac{\mathrm{i}\pi(k_o\ell\sin\psi)^2}{8}\right)\right\}\sqrt{\ell^2 - y_1^2}.$$

Because $\mathscr{A} \propto \mathrm{e}^{-\mathrm{i}k_3y_3} = \mathrm{e}^{-\mathrm{i}k_o y_3\cos\psi}$, it now follows from equation (5.7) that

$$\begin{aligned} \mathscr{V} &= \frac{\mathrm{i}(\pi\rho_o\ell/2m)\mathscr{A}k_o\cos\Theta}{Dk_o^4\cos{}^4\psi/m\omega^2 - (1 + \pi\rho_o\ell/2m[1 + \mathrm{i}\pi(k_o\ell\sin\psi)^2/8])}, \\ &= \frac{\mathrm{i}\beta\mathscr{A}k_o\cos\Theta}{(1-\mathrm{i}\mu)\omega^2\cos^4\psi/\omega_c^2 - (1 + \beta[1 + \mathrm{i}\pi(k_o\ell\sin\psi)^2/8])}. \end{aligned} \tag{5.8}$$

Here a complex stiffness $D = D_o(1 - \mathrm{i}\mu)$ has been introduced, where D_o is real and $\mu \ll 1$ is a suitable *loss factor*; also $\omega_c = c_o^2\sqrt{m/D_o}$ is the coincidence frequency of the plate, and $\beta = \rho_o\pi\ell/2m$ is the ratio of the added mass to the mass of the plate.

The periodic motion of the plate at speed $\mathscr{V}$ produces a locally incompressible motion of fluid past the stationary airfoil in the y_2-direction. At source positions $\mathbf{y}$ near the airfoil we can therefore write, to leading order,

$$G(\mathbf{x}, \mathbf{y}, \omega) \approx G'_{\mathrm{o}} + \mathscr{V} X_2(\mathbf{y}), \tag{5.9}$$

where $X_2(\mathbf{y})$ is the potential function discussed in Section 3 that satisfies conditions (3.3) on the airfoil and plate, and $G'_{\mathrm{o}} \sim G_{\mathrm{o}}$ is smoothly varying near the airfoil,

The term in X_2 in equation (5.9) governs the sound produced by the interaction of the airfoil with boundary-layer turbulence in the presence of the elastic plate; contributions to the radiation from the component G'_{o}, whose length scale of variation is large compared to the airfoil chord, will tend to be of lower, quadrupole order, and may be ignored at very low Mach numbers. Thus, for the purpose of computing the sound generated by small-scale turbulence interacting with the airfoil, we can take (using definition (5.5) of $\mathscr{A}$)

$$G(\mathbf{x}, \mathbf{y}, \omega) \approx \frac{-\mathrm{i}\beta k_{\mathrm{o}} X_2(\mathbf{y}) \cos\Theta\, \mathrm{e}^{\mathrm{i}k_{\mathrm{o}}(|\mathbf{x}| - y_3\cos\psi)}}{4\pi|\mathbf{x}|\{(1-\mathrm{i}\mu)\omega^2\cos^4\psi/\omega_{\mathrm{c}}^2 - (1+\beta[1+\mathrm{i}\pi(k_{\mathrm{o}}\ell\sin\psi)^2/8])\}}, \quad |\mathbf{x}| \to \infty. \tag{5.10}$$

5.2. The Acoustic Spectrum

Consider now the production of sound by turbulence impinging on an airfoil modeled by the two-dimensional strip of Figure 5(a). The solution $B(\mathbf{x}, \omega)$ of the time harmonic form of equation (5.1),

$$(\nabla^2 + k_{\mathrm{o}}^2)B = -\operatorname{div}(\boldsymbol{\Omega} \wedge \mathbf{v})(\mathbf{x}, \omega) \tag{5.11}$$

and Green's function $G(\mathbf{x}, \omega)$ satisfy the same linear boundary conditions on the airfoil and plate. Green's theorem therefore supplies, by the usual procedure [see, e.g. Howe 1998], the representation

$$B(\mathbf{x}, \omega) = \int \frac{\partial G(\mathbf{x}, \mathbf{y}, \omega)}{\partial \mathbf{y}} \cdot (\boldsymbol{\Omega} \wedge \mathbf{v})(\mathbf{y}, \omega)\, \mathrm{d}^3\mathbf{y}.$$

In the far field the acoustic pressure $p = \rho_{\mathrm{o}} B$, so that in the low-frequency regime where equation (5.10) is applicable we have

$$p(\mathbf{x}, \omega) \approx \frac{-\mathrm{i}\rho_{\mathrm{o}}\beta k_{\mathrm{o}} \cos\Theta\, \mathrm{e}^{\mathrm{i}k_{\mathrm{o}}|\mathbf{x}|}}{4\pi|\mathbf{x}|\{(1-\mathrm{i}\mu)\omega^2\cos^4\psi/\omega_{\mathrm{c}}^2 - (1+\beta[1+\mathrm{i}\pi(k_{\mathrm{o}}\ell\sin\psi)^2/8])\}}$$
$$\times \int (\nabla X_2 \cdot \boldsymbol{\Omega} \wedge \mathbf{v})(\mathbf{y}, \omega)\mathrm{e}^{-\mathrm{i}k_{\mathrm{o}}y_3\cos\psi}\mathrm{d}^3\mathbf{y}. \tag{5.12}$$

To evaluate the integral we note first that, for acoustically compact turbulent sources, the argument of the exponential in the integrand is effectively constant over distances of order U/ω, the correlation scale of the turbulence fluctuations of frequency ω. This means that the incompressible equation (3.5) can be applied locally to express the sound in terms of the upwash velocity. When the chord $2a \gg \delta$ the upwash velocity can be approximated by the component v_2 of the impinging boundary-layer velocity fluctuations, which can be represented as the Fourier integral

$$v_2(x_1, x_3, \omega) = \iint_{-\infty}^{\infty} \hat{v}_2(\kappa_1, \kappa_3, \omega)\mathrm{e}^{\mathrm{i}(\kappa_1 y_1 + \kappa_3 y_3)}\,\mathrm{d}\kappa_1\,\mathrm{d}\kappa_3, \tag{5.13}$$

where both the velocity and its Fourier transform $\hat{v}_2(\kappa_1, \kappa_3, \omega)$ are regarded as evaluated at the airfoil stand-off distance h from the plate. We then find, by the procedure leading to equations (2.16) and (4.12), that the acoustic pressure can be written

$$p(\mathbf{x}, \omega) \approx \frac{\rho_o \beta \omega^2 \sqrt{2\pi a} \cos\Theta\, e^{i(k_o|\mathbf{x}| + \pi/4)}}{2c_o|\mathbf{x}|\{(1 - i\mu)\,\omega^2 \cos^4\psi/\omega_c^2 - (1 + \beta[1 + i\pi(k_o \ell \sin\psi)^2/8])\}}$$
$$\times f\left(\frac{a}{h}\right)\int_{-\infty}^{\infty} \frac{\hat{v}_2(\kappa_1, k_o\cos\psi, \omega)e^{i\kappa_1 a}\,d\kappa_1}{(\kappa_1 - i0)^{3/2}}, \qquad |\mathbf{x}| \to \infty. \tag{5.14}$$

Now, let $\Psi(\kappa_1, \kappa_2, \omega)$ denote the wavenumber–frequency spectrum of the upwash velocity v_2 (at $x_2 = h$), and introduce the frequency spectrum $\Phi(\mathbf{x}, \omega)$ of the acoustic pressure at the far-field observation point $\mathbf{x}$, defined such that

$$\langle p^2(\mathbf{x}, t)\rangle = \int_{-\infty}^{\infty} \Phi(\mathbf{x}, \omega)\,d\omega,$$

where the angle brackets $\langle\rangle$ represent an ensemble average. Then

$$\langle p(\mathbf{x}, \omega)p^*(\mathbf{x}, \omega')\rangle = \delta(\omega - \omega')\Phi(\mathbf{x}, \omega),$$
$$\langle \hat{v}_2(\kappa_1, k_3, \omega)\hat{v}_2^*(\kappa'_1, k_3, \omega')\rangle = \frac{L}{2\pi}\delta(\omega - \omega')\delta(\kappa_1 - \kappa'_1)\Psi(\kappa_1, k_3, \omega), \tag{5.15}$$

where the asterisk denotes the complex conjugate, and $L \gg \delta$ is the spanwise extent of the turbulent flow. Hence,

$$\Phi(\mathbf{x}, \omega) \approx \left(\frac{La}{4c_o^2|\mathbf{x}|^2}\right) \frac{\rho_o^2\beta^2 f^2\, \omega^4 \cos^2\Theta}{\{(\omega^2\cos^4\psi/\omega_c^2 - (1 + \beta))^2 + \omega^4/\omega_c^4(\mu\cos^4\psi + \pi\beta\omega_c^2\ell^2\sin^2\psi/8c_o^2)^2\}}$$
$$\times \int_{-\infty}^{\infty} \frac{\Psi(\kappa_1, k_o\cos\psi, \omega)\,d\kappa_1}{|\kappa_1|^3} \qquad |\mathbf{x}| \to \infty, \tag{5.16}$$

where $f \equiv f(a/h)$.

5.3. Approximate Representation of the Sound

By analogy with the boundary-layer wall pressure spectrum (Chase 1980), the velocity spectrum $\Psi(\kappa_1, \kappa_3, \omega)$ is expected to have a large peak in the vicinity of a "convective ridge" centered on $\kappa_1 \sim \omega/U_c$, $\kappa_3 \sim 0$, where $U_c \sim 0{\cdot}7U$ is an eddy convection velocity. Also, because $k_o\delta \ll 1$ we can take $\Psi(\kappa_1, k_o\cos\psi, \omega) = \Psi(\kappa_1, 0, \omega)$. Thus, in a first approximation

$$\int_{-\infty}^{\infty} \frac{\Psi(\kappa_1, k_o\cos\psi, \omega)\,d\kappa_1}{|\kappa_1|^3} \sim \frac{\ell_3\Phi_{22}(\omega)}{(\omega/U_c)^3},$$

where $\Phi_{22}(\omega)$ is the frequency spectrum of the normal velocity v_2 at distance h from the wall, and $\ell_3 = \int_0^\infty \mathcal{R}_{22}(y_3, \omega)\,dy_3$ is the spanwise x_2-velocity correlation length at frequency ω, $\mathcal{R}_{22}(y_3, \omega)$ being the spanwise correlation function normalized such that $\mathcal{R}_{22}(0, \omega) = 1$.

Equation (5.16) can therefore be approximated by

$$\Phi(\mathbf{x}, \omega) \approx \left(\frac{La}{4|\mathbf{x}|^2}\right) \frac{\rho_o^2 U_c^2 M_c^2 \beta^2 f^2 \cos^2\Theta(\omega\ell_3/U_c)\Phi_{22}(\omega)}{\{(\omega^2\cos^4\psi/\omega_c^2 - (1 + \beta))^2 + \omega^4/\omega_c^4(\mu\cos^4\psi + \pi\beta\omega_c^2\ell^2\sin^2\psi/8c_o^2)^2\}}$$
$$|\mathbf{x}| \to \infty, \tag{5.17}$$

where $M_c = U_c/c_o$.

In applications it will usually be permissible to simplify this result further, because the assumption that the plate width 2ℓ is smaller than an acoustic wavelength is generally valid only for $\omega \ll \omega_c$. For example, in the case of a steel plate in water of thickness $\Delta \ll \ell$, the coincidence frequency satisfies $\omega_c \Delta / c_o \approx 0{\cdot}95$, so that

$$\frac{\omega}{\omega_c} = \left(\frac{\omega \ell}{c_o}\right)\left(\frac{c_o}{\omega_c \Delta}\right)\frac{\Delta}{\ell} \ll 1.$$

Equation (5.17) therefore reduces to

$$\Phi(\mathbf{x}, \omega) \approx \left(\frac{La \cos^2 \Theta}{4|\mathbf{x}|^2}\right)\frac{\beta^2 f^2}{(1+\beta)^2}\,\rho_o^2 U_c^2 M_c^2 \left(\frac{\omega \ell_3}{U_c}\right)\Phi_{22}(\omega), \qquad |\mathbf{x}| \to \infty. \tag{5.18}$$

Furthermore, the transverse correlation length $\ell_3 \sim U/\omega$ (Chase 1980), so that $\omega \ell_3 / U_c$ probably varies very slowly with frequency. Equation (5.18) accordingly suggests that the acoustic pressure frequency spectrum $\Phi(\mathbf{x}, \omega) \propto \Phi_{22}(\omega)$, the frequency spectrum of the normal component of velocity in the boundary layer at the airfoil stand-off distance h. When $\beta \gg 1$ the inertia of the plate is negligible in the acoustic domain, and equation (5.18) then reduces to the corresponding prediction for an isolated airfoil, except for the correction factor $f(a/h)$ that governs the influence of the plate on the airfoil lift force.

6. CONCLUSION

The unsteady surface force F_i exerted on a stationary rigid body immersed in an incompressible turbulent stream can be expressed in terms of a surface integral over the body involving the *upwash* velocity induced by the free vorticity $\boldsymbol{\Omega}$ and a harmonic function X_i that depends only on the shape of the body. The upwash velocity is calculated using the Biot–Savart formula for the velocity induced by $\boldsymbol{\Omega}$ when the presence of the body is ignored, although $\boldsymbol{\Omega}$ must first be found by taking explicit account of the interaction of the body with the turbulent stream. The function X_i may be interpreted as the velocity potential of incompressible flow past the body that has unit speed in the i-direction at large distances from the body. For wall turbulent boundary layer flows, the unsteady *lift* experienced by a body in the x_2-direction normal to the wall is given by the same formula provided X_2 is redefined to represent potential flow past the body produced by motion of the wall at unit speed towards the body, and provided the Biot–Savart velocity field is augmented by the velocity induced by a distribution of image vorticity in the wall.

For slender, airfoil-shaped bodies, when the turbulence length scales are small compared to the streamwise extent of the body (such as the airfoil chord), vortex shedding into the wake (in accordance with some sort of *Kutta* condition) tends to reduce the magnitude of the upwash fluctuations in trailing edge regions. The main contributions to the surface integral for the force then come from the nose regions, where the upwash velocity may be approximated by the undisturbed velocity of the impinging turbulent flow. Analytical results based on this approximation for a thin plate airfoil of chord $2a$ in a boundary layer at distance h from the wall show that the amplitude of the lift force increases as a/h increases, and that ultimately the force becomes independent of a and scales with the ratio of h to the hydrodynamic wavelength. The lift force on an isolated airfoil in a very low Mach number flow is equivalent to a relatively strong acoustic source of *dipole* type. The dipole strength is reduced to zero if the airfoil is placed in a boundary layer over a *rigid* wall. However, a real wall often becomes compliant over length scales comparable to the characteristic acoustic wavelength, so that in practice the dipole remains finite; a typical case of this kind has been discussed in Section 5.

References

Abramowitz, M. & Stegun, I. A. (eds). 1970 *Handbook of Mathematical Functions*, 9th corrected printing. US Department of Commerce, National Bureau of Standards Applied Mathematics Series No.55.

Amiet, R. & Sears, W. R. 1970 The aerodynamic noise of small-perturbation subsonic flows. *Journal of Fluid Mechanics* **44,** 227–235.

Atassi, H. M. 1984 The Sears problem for a lifting airfoil revisited—new results. *Journal of Fluid Mechanics* **141,** 109–122.

Batchelor, G. K. 1967 *An Introduction to Fluid Dynamics*. Cambridge: Cambridge University Press.

Chase, D. M. 1980 Modeling the wavevector-frequency spectrum of turbulent boundary layer wall pressure. *Journal of Sound and Vibration* **70,** 29–67.

Crighton, D. G. 1985 The Kutta condition in unsteady flow. *Annual Reviews of Fluid Mechanics* **17,** 411–445.

Curle, N. 1955 The influence of solid boundaries upon aerodynamic sound. *Proceedings of the Royal Society of London A* **231,** 505–514.

Dowling, A. P. 1989 The effect of large-eddy breakup devices on flow noise. *Journal of Fluid Mechanics* **208,** 193–223.

Filotas, L. T. 1973 Vortex induced helicopter blade loads and noise. *Journal of Sound and Vibration* **27,** 387–398.

Gebert, G. A. & Atassi, H. M. 1989 Unsteady vortical disturbances around a thin airfoil in the presence of a wall. *AIAA Journal* **27,** 1448–1450.

Glegg, S. A. L. 1989 Sound radiation from an airfoil encountering an oblique gust in its plane of motion. *AIAA Journal* **27,** 1820–1822.

Goldstein, M. E. & Atassi, H. M. 1976 A complete second order theory for the unsteady flow about an airfoil due to a periodic gust. *Journal of Fluid Mechanics* **74,** 741–765.

Howe, M. S. 1976 The influence of vortex shedding on the generation of sound by convected turbulence. *Journal of Fluid Mechanics* **76,** 711–740.

Howe, M. S. 1989*a* On unsteady surface forces, and sound produced by the normal chopping of a rectilinear vortex. *Journal of Fluid Mechanics* **206,** 131–153.

Howe, M. S. 1989*b* Structural and acoustic noise generated by a large-eddy breakup device. *Proceedings of the Royal Society of London A* **424,** 461–486.

Howe, M. S. 1998 *Acoustics of Fluid–Structure Interactions* Cambridge: Cambridge University Press.

Ivanov, V. I. & Trubetskov, M. K. 1995 *Handbook of Conformal Mapping with Computer-Aided Visualization*. Boca Raton, FL: CRC Press.

Junger, M. C. & Feit, D. 1993 *Sound, Structures and their Interactions*. New York: Acoustical Society of America.

Lamb, H. 1932 *Hydrodynamics*, 6th edition. Cambridge: Cambridge University Press (reprinted 1993).

Lighthill, M. J. 1952 On sound generated aerodynamically. Part I: general theory. *Proceedings of the Royal Society of London A* **211,** 564–587.

Marshall, J. S. & Grant, J. R. 1996 Penetration of a blade into a vortex core: vorticity response and unsteady blade forces. *Journal of Fluid Mechanics* **308,** 83–110.

Milne-Thomson, L. M. 1968 *Theoretical Hydrodynamics*, 5th edition. London: Macmillan.

Mugridge, B. D. 1971 Gust loading of a thin airfoil. *Aeronautical Quarterly* **xx,** 301–310.

Sears, W. R. 1941 Some aspects of non-stationary airfoil theory and its practical applications. *Journal of the Aeronautical Sciences* **8,** 104–108.

Widnall, S. 1971 Helicopter noise due to blade–vortex interaction. *Journal of the Acoustical Society of America* **50,** 354–365.